Nucleon axial and electromagnetic FFs from Lattice QCD simulations at the physical point

Extended Twisted Mass Collaboration

Dr. Simone Bacchio

Computational Scientist
CaSToRC, The Cyprus Institute
National Competence Center in HPC

05/08/24 - ECT*, Trento

Co-funded by the European Union

Republic of Cyprus

RESEARCH & INNOVATION FOUNDATION

INNO4 SCALE

EuroHPC Joint Undertaking

Motivation: Neutrino oscillation experiments

Monte-Carlo simulation needs input on the differential cross section to reconstruct the energy of the neutrino from the momentum of the detected charged lepton.

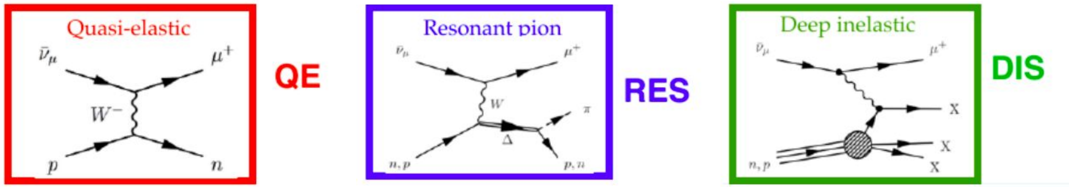

We focus on quasi-elastic scattering providing first-principle predictions on axial form factors

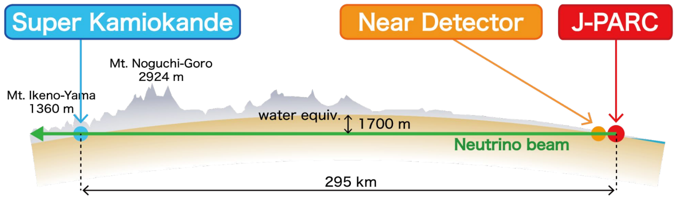

T2K: Tokai to Super-Kamiokande
E = 0.6 GeV, L/E ≂ 500 km/GeV.

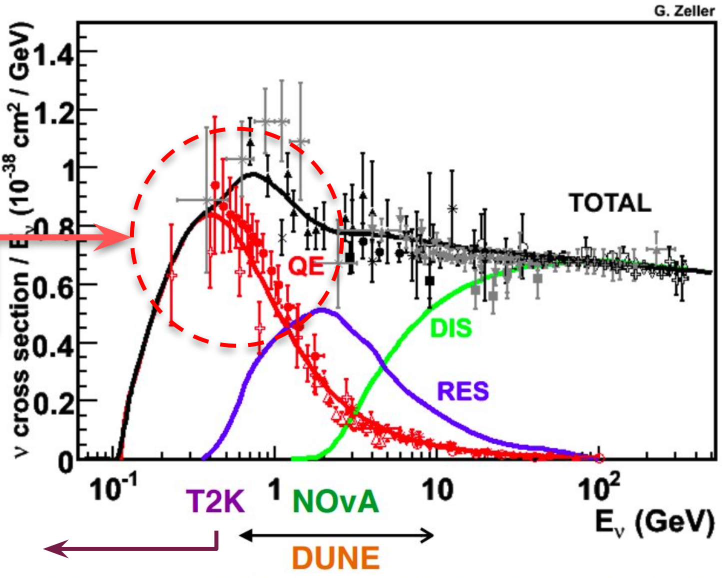

J.A. Formaggio, G. Zeller, Reviews of Modern Physics, 84 (2012)

The weak axial-vector matrix element

The transition matrix element of the neutron β-decay is

$$\mathcal{M}(n \to p\, e^-\, \bar{\nu}_e) = \frac{G_F}{\sqrt{2}} V_{ud} \sum_\mu \underbrace{\langle p(p') | W_\mu | n(p) \rangle}\, L_\mu$$

with
$$W_\mu = V_\mu - A_\mu$$
$$V_\mu = \bar{u}\gamma_\mu d$$
$$A_\mu = \bar{u}\gamma_\mu\gamma_5 d$$

Vector contributions are well determined experimentally from lepton-nucleon scattering

Axial-vector matrix element $\langle p(p') | A_\mu | n(p) \rangle$

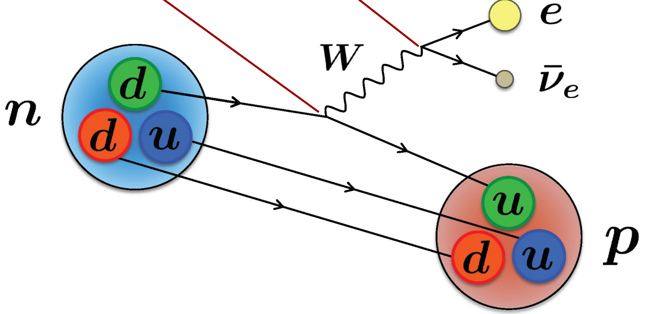

Neutrino-nucleon scattering processes are related to matrix elements at finite momentum transfer.

The axial and induced pseudoscalar FF

Neglecting isospin-breaking effects, transition FFs are equivalent to isovector FFs

$$\langle p(p')|A_\mu|n(p)\rangle \qquad \xrightarrow[u=d]{} \qquad \langle N(p')|A_\mu^{\text{isov}}|N(p)\rangle$$

$$A_\mu = \bar{u}\gamma_\mu\gamma_5 d \qquad\qquad A_\mu^{\text{isov}} = \bar{u}\gamma_\mu\gamma_5 u - \bar{d}\gamma_\mu\gamma_5 d$$

Matrix elements are decomposed into Lorentz-invariant form factors (FF)

$$\langle N(p',s')|A_\mu|N(p,s)\rangle = \bar{u}_N(p',s')\left[\gamma_\mu G_A(Q^2) - \frac{Q_\mu}{2m_N}G_P(Q^2)\right]\gamma_5 u_N(p,s),$$

Axial FF *Induced pseudoscalar FF*

How to? Lattice QCD Simulations

$$\langle \mathcal{O} \rangle = \frac{1}{Z} \int \mathcal{D}[U] \mathcal{O}(D_f^{-1}[U], U) \left(\prod_{f=u,d,s,c} \mathrm{Det}(D_f[U]) \right) e^{-S_{QCD}[U]}$$

1

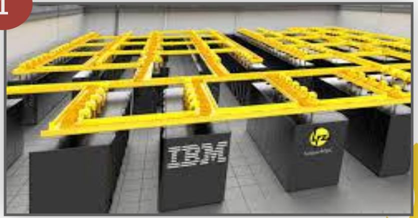

2

3

Simulation

- Markov chain Monte Carlo to generate ensembles of gluon-field configurations {U}

$$P[U] = \frac{1}{Z} \left(\prod_{f=u,d,s,c} \mathrm{Det}(D_f[U]) \right) e^{-S_{QCD}[U]}$$

Analysis

- Construction of hadron correlation functions on background field configurations:

$$\langle N(p', s') | \mathcal{O} | N(p, s) \rangle$$

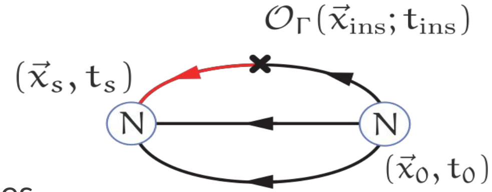

Data analysis – post-processing

- Statistical analysis, resampling, derived quantities
- <u>Excited state contamination</u> and stochastic errors
- <u>Continuum</u> and infinite volume extrapolation

Ensembles

Landscape of ensembles used for nucleon structure:

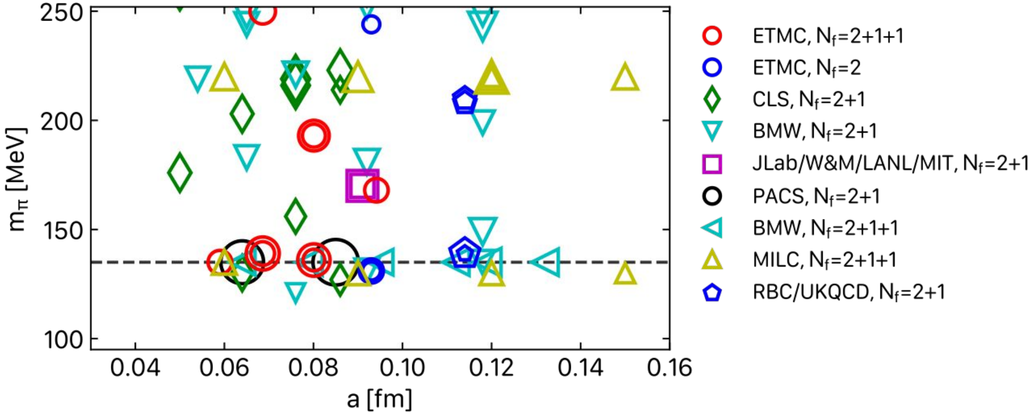

Ensembles by ETMC

Landscape of ensembles used for nucleon structure:

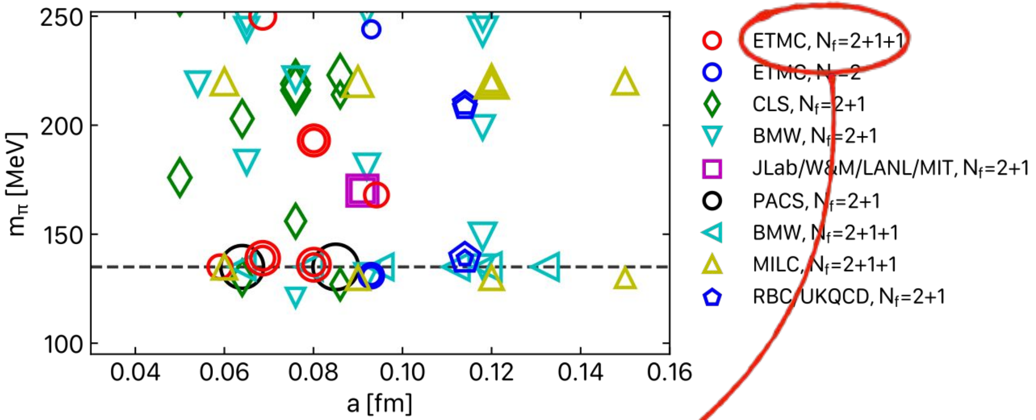

ETMC: three N_f=2+1+1 ensembles at physical pion mass

Ens. ID (abbrv.)	Vol.	a [fm]
cB211.072.64 (cB64)	64×128	0.080
cC211.060.80 (cC80)	80×160	0.068
cD211.054.96 (cD96)	96×192	0.057

- Three lattice spacings at physical point
- Ongoing generation of finer ensembles and larger volumes
- ***This talk:*** 3 ensembles with: a = 0.057 - 0.08 fm

Nucleon two-point functions

$$G(t_s) = \sum_{\vec{x}} P_0^{\alpha\beta} \langle \bar{\chi}_N^{\beta}(\vec{x}_s, t_s) | \chi_N^{\alpha}(\vec{0}, 0) \rangle = \sum_k c_k e^{-t_s E_k}$$

with $\chi_N^{\alpha}(x) = \epsilon^{abc} u_{\alpha}^{a}(x) [u^b(x) C\gamma_5 d^c(x)]$

- Two-point functions
  - Ground state dominance at large-time limit $G(t_s) = c_0^{-t_s m_N}\big|_{t_s \to \infty}$
  - Error increases exponentially with t
  - Density of excited states increases with volume

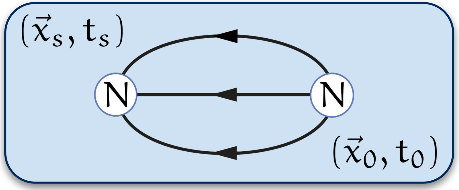

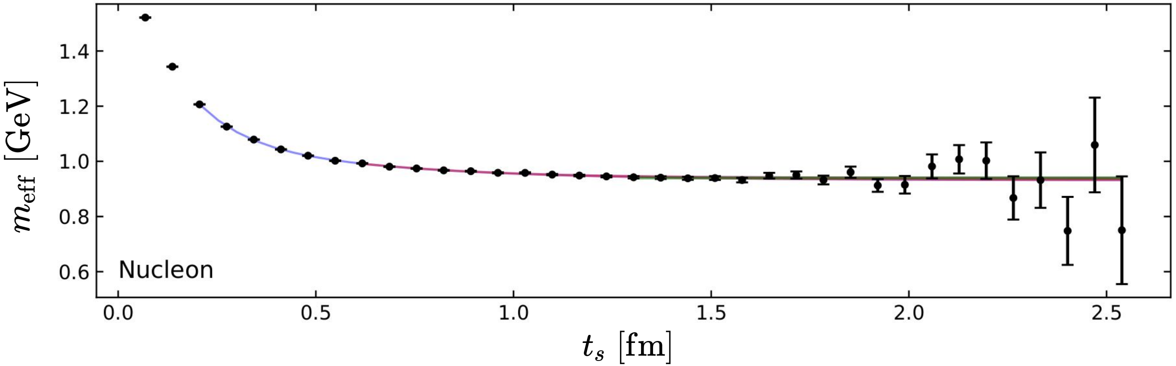

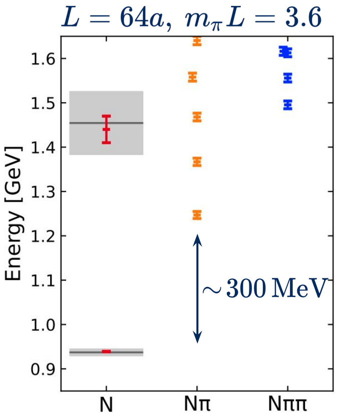

Nucleon three-point functions

$$G_\Gamma(P;\vec{q};t_s,t_{\rm ins}) = \sum_{\vec{x}_s,\vec{x}_{\rm ins}} e^{-i\vec{q}\cdot\vec{x}_{\rm ins}} P^{\alpha\beta} \langle \bar{\chi}^\beta_N(\vec{x}_s,t_s)|\mathcal{O}_\Gamma(\vec{x}_{\rm ins},t_{\rm ins})|\chi^\alpha_N(\vec{0},0)\rangle$$

suitable projector

e.g. $\mathcal{O}_A(x) = \bar{\psi}(x)\gamma_5\gamma^\mu\psi(x)$

- Three-point functions
  - Ground state at $t_s \to \infty$, $(t_s - t_{\rm ins}) \to \infty$
  - Error increases exponentially with t_s
  - Statistics increased to keep errors constant

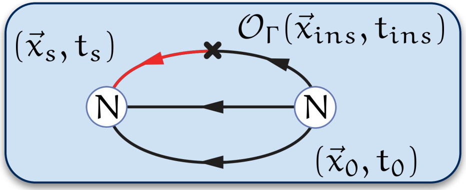

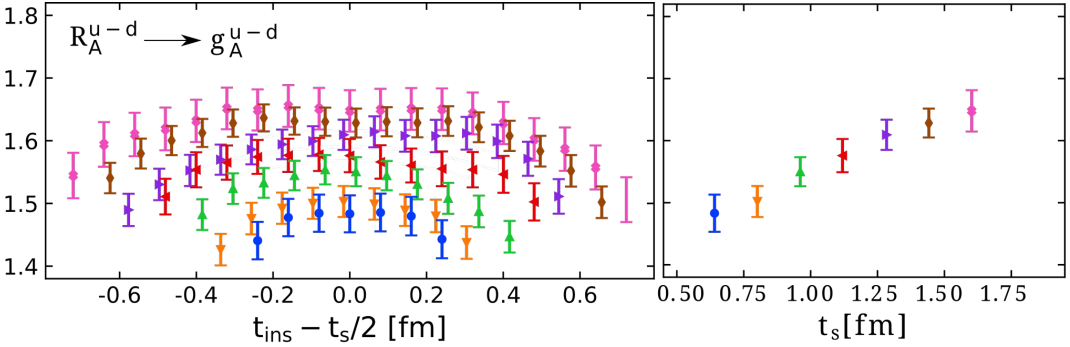

$\times 750$ configurations

t_s/a	t_s[fm]	n_{src}
8	0.64	1
10	0.80	2
12	0.96	5
14	1.12	10
16	1.28	32
18	1.44	112
20	1.60	128
Nucleon 2pt		477

~30M inversions!

Nucleon three-point functions

$$G_\Gamma(P;\vec{q};t_s,t_{ins}) = \sum_{\vec{x}_s,\vec{x}_{ins}} e^{-i\vec{q}\cdot\vec{x}_{ins}} P^{\alpha\beta} \langle \bar{\chi}_N^\beta(\vec{x}_s,t_s)|\mathcal{O}_\Gamma(\vec{x}_{ins},t_{ins})|\chi_N^\alpha(\vec{0},0)\rangle$$

$$G_\Gamma(t_s,t_{ins}) \simeq A_{00}e^{-m_N t_s} + A_{01}\left(e^{-E_1 t_{ins}} + e^{-E_1 t_s + (E_1 - m_N)t_{ins}}\right) + A_{11}e^{-E_1 t_s}$$

$$G(t) \simeq c_0 e^{-m_N t_s} + c_1 e^{-E_1 t_s}$$

Desired matrix element: $\mathcal{M} = \dfrac{A_{00}}{c_0}$

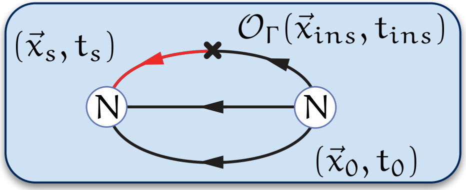

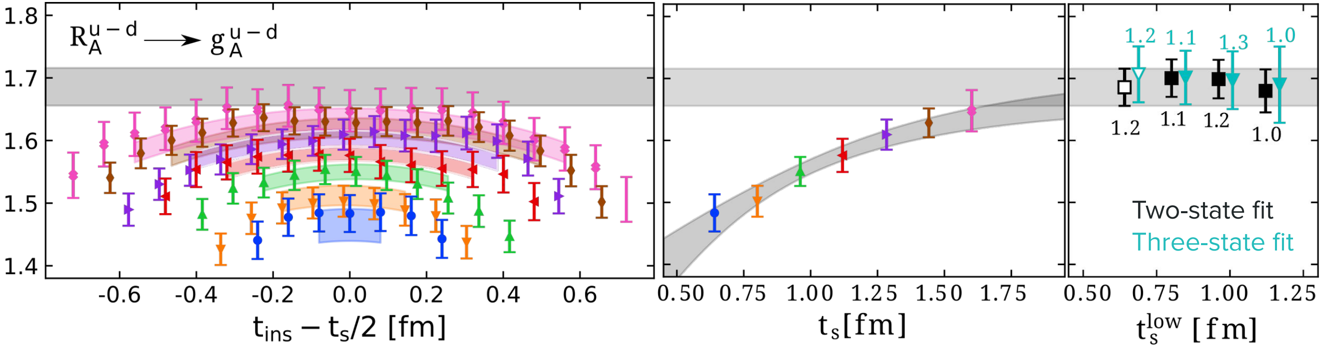

$\times 750$ configurations

t_s/a	t_s[fm]	n_{src}
8	0.64	1
10	0.80	2
12	0.96	5
14	1.12	10
16	1.28	32
18	1.44	112
20	1.60	128
Nucleon 2pt		477

~30M inversions!

[C. Alexandrou, S. B., et al. "Nucleon axial, tensor, and scalar charges and σ-terms in lattice QCD". Phys. Rev., D102(5):054517, 2020]

The three ensembles and model averaging

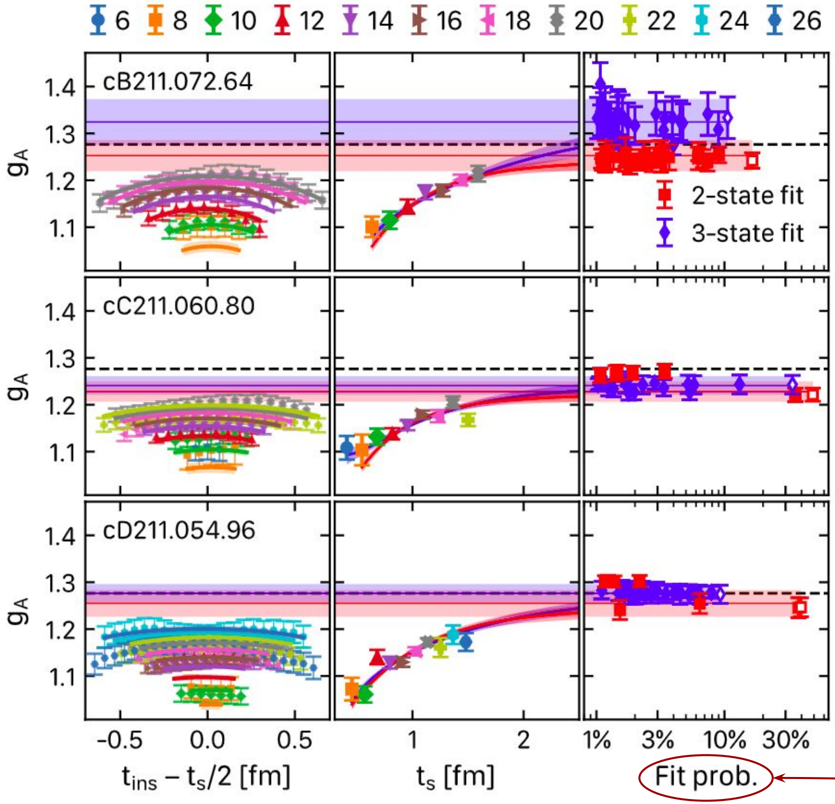

Ensemble	V/a^4	β	a [fm]	m_π [MeV]	$m_\pi L$
cB211.072.64	$64^3 \times 128$	1.778	0.07957(13)	140.2(2)	3.62
cC211.060.80	$80^3 \times 160$	1.836	0.06821(13)	136.7(2)	3.78
cD211.054.96	$96^3 \times 192$	1.900	0.05692(12)	140.8(2)	3.90

cB211.072.64		
750 configurations		
t_s/a	t_s[fm]	n_{src}
8	0.64	1
10	0.80	2
12	0.96	5
14	1.12	10
16	1.28	32
18	1.44	112
20	1.60	128
Nucleon 2pt		477

cC211.060.80		
400 configurations		
t_s/a	t_s[fm]	n_{src}
6	0.41	1
8	0.55	2
10	0.69	4
12	0.82	10
14	0.96	22
16	1.10	48
18	1.24	45
20	1.37	116
22	1.51	246
Nucleon 2pt		650

cD211.054.96		
500 configurations		
t_s/a	t_s[fm]	n_{src}
8	0.46	1
10	0.57	2
12	0.68	4
14	0.80	8
16	0.91	16
18	1.03	32
20	1.14	64
22	1.25	16
24	1.37	32
26	1.48	64
Nucleon 2pt		480

Up to 1.5fm for all ensembles

Model average over thousands of fits: $\log(w_i) = -\frac{\chi_i^2}{2} + N_{\mathrm{dof},i}$

$p_i = \frac{w_i}{Z}$ with $Z = \sum_i w_i$. [E. T. Neil, J. W. Sitison, arXiv:2208.14983]

… and at finite momentum transfer

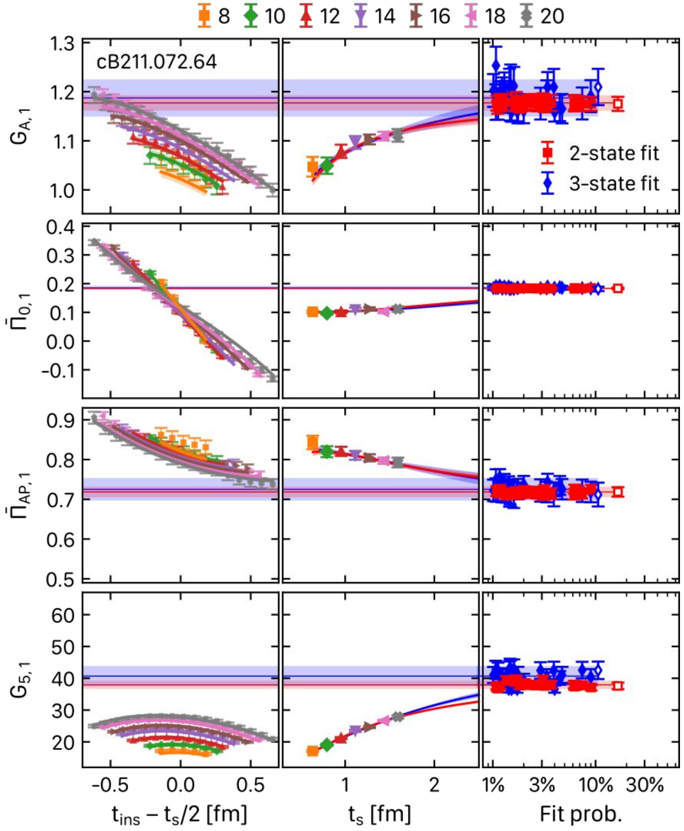

$$\Pi_\mu(\Gamma_k;\vec{q}) = \frac{\mathcal{A}_\mu^{0,0}(\Gamma_k,\vec{q})}{\sqrt{c_0(\vec{0})c_0(\vec{q})}}$$

Three-point ground state

Two-point ground state

Combined fit of all three-point functions at the same Q^2

$$\Pi_i(\Gamma_k,\vec{q}) = \frac{i\mathcal{K}}{4m_N}\left[\frac{q_k q_i}{2m_N}G_P(Q^2) - \delta_{i,k}(m_N+E_N)G_A(Q^2)\right]$$

$$\Pi_0(\Gamma_k,\vec{q}) = -\frac{q_k\mathcal{K}}{2m_N}\left[G_A(Q^2) + \frac{(m_N-E_N)}{2m_N}G_P(Q^2)\right]$$

$$\Pi_5(\Gamma_k,\vec{q}) = -\frac{iq_k\mathcal{K}}{2m_N}G_5(Q^2) \longrightarrow \textit{Pseudoscalar FF}$$

Comparing two- and three-state fit FFs

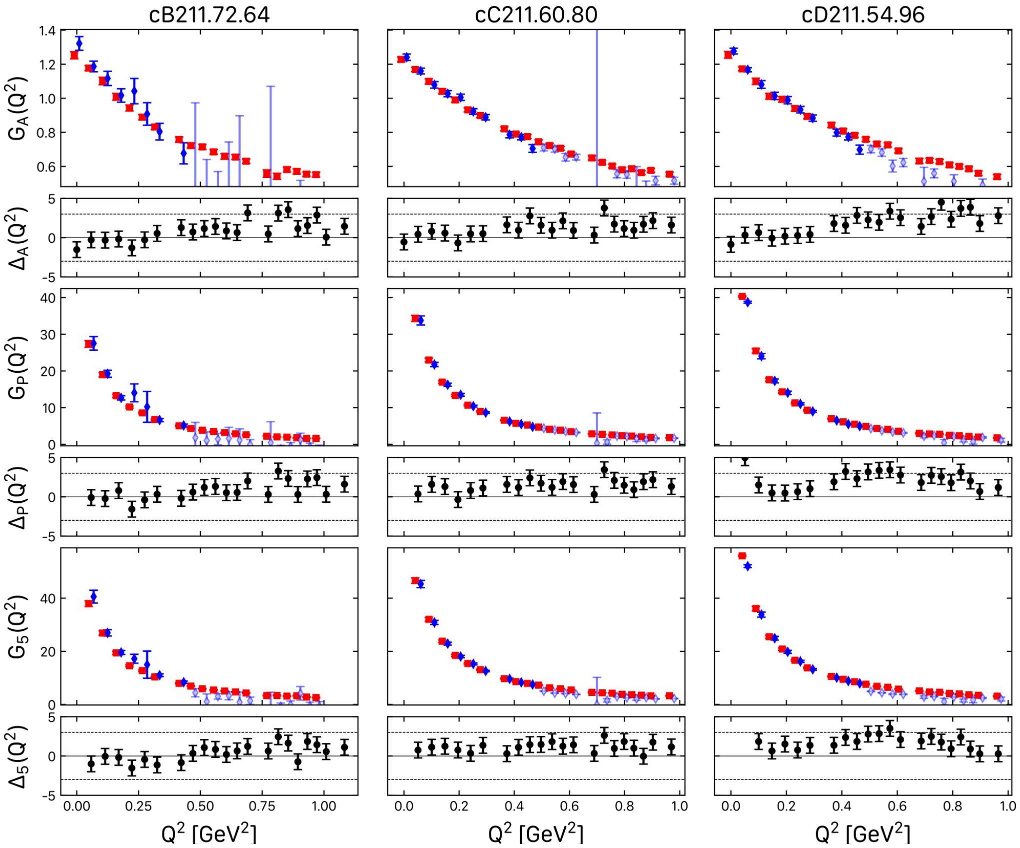

- Most values compatible within 3σ
- Combined fit of Q^2 and a^2 dependence

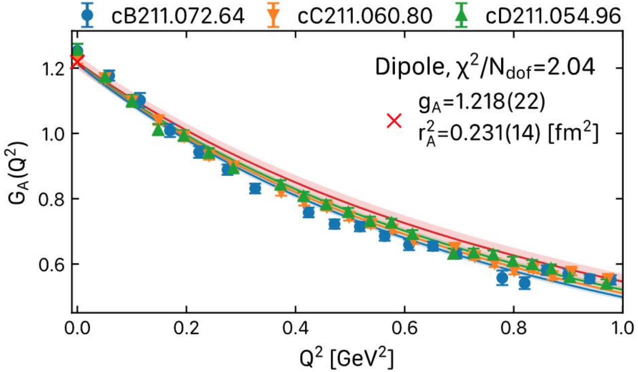

$$G(Q^2, a^2) = \frac{g(a^2)}{(1+\frac{Q^2}{12} r^2(a^2))^2} \qquad g(a^2) = g_0 + a^2 g_2 \qquad r^2(a^2) = r_0^2 + a^2 r_2^2$$

Dipole vs z-expansion

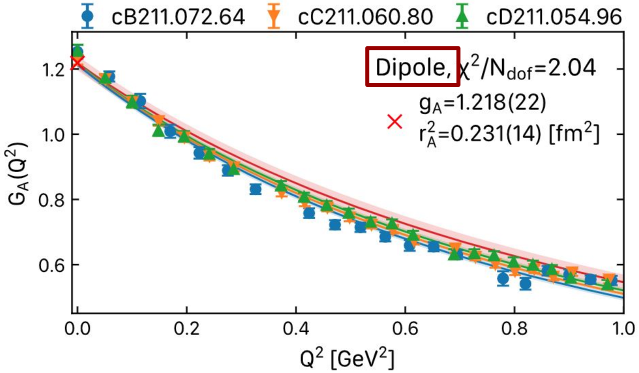

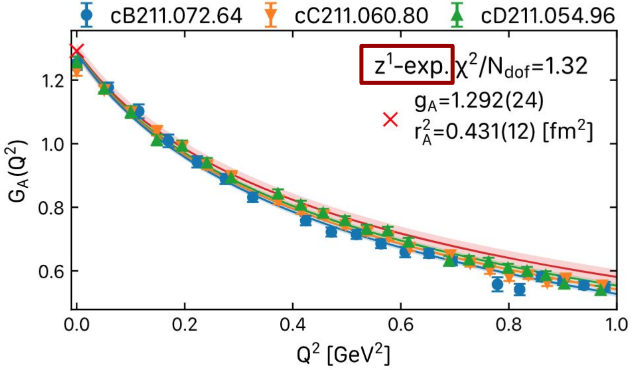

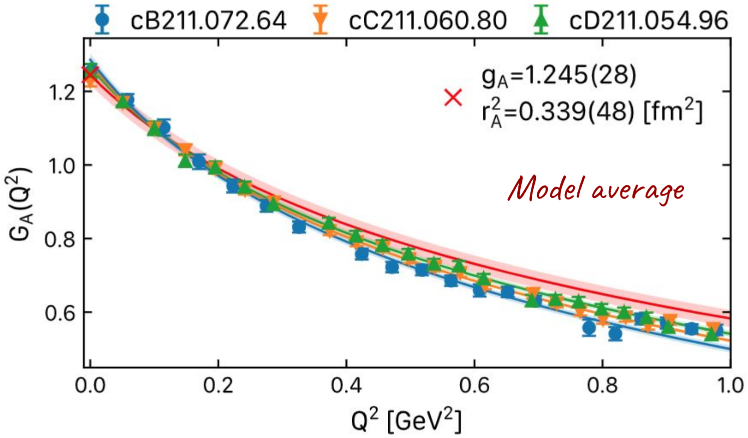

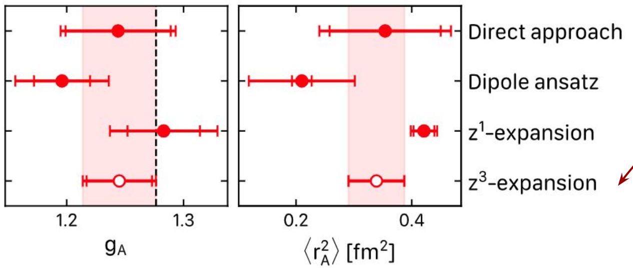

Compatible with the direct approach but smaller error because all information used

Comparison with other studies

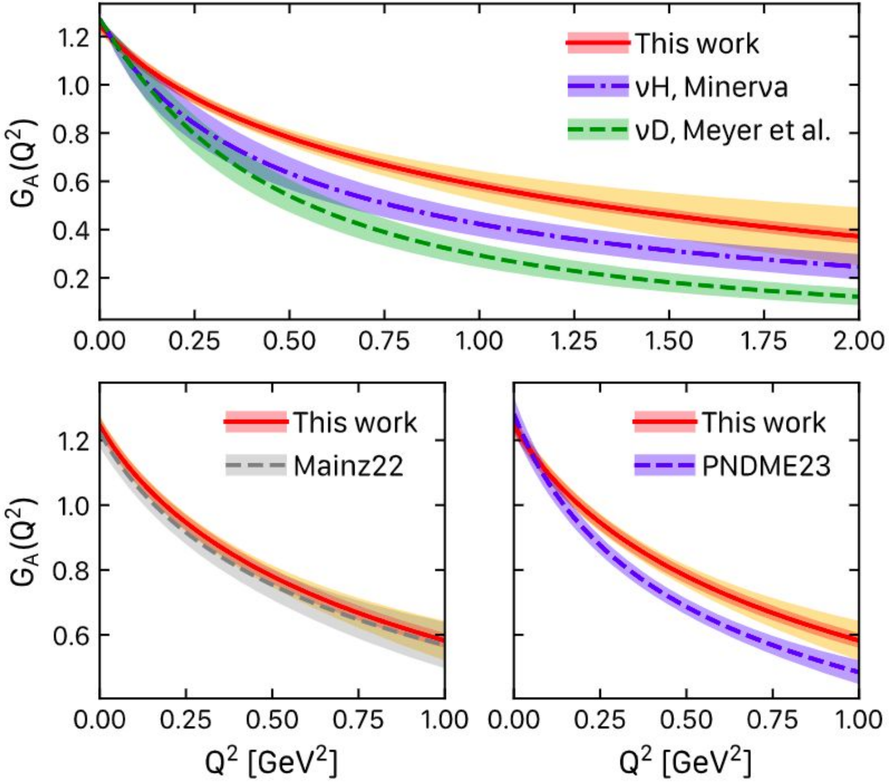

- Overall good agreement between recent lattice results and better agreement with the very recent results from Minerva

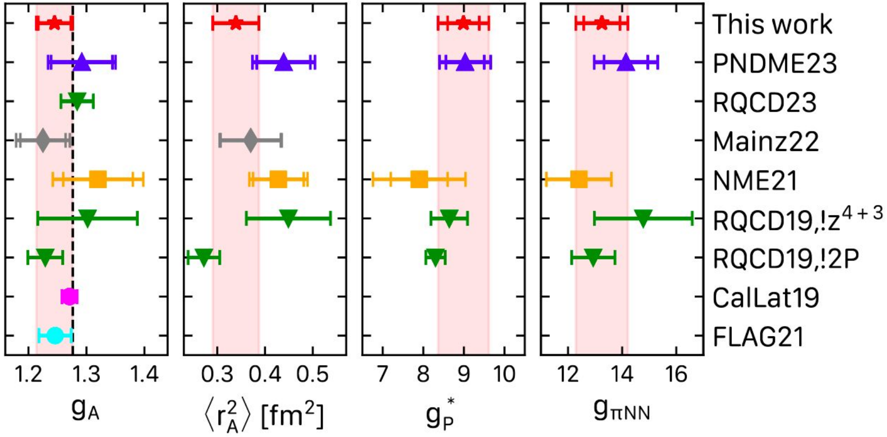

Pseudoscalar FF and operator relations

Axial FFs are commonly studied together with the pseudoscalar FF

$$\langle N(p',s')|A_\mu|N(p,s)\rangle = \bar{u}_N(p',s')\left[\gamma_\mu G_A(Q^2) - \frac{Q_\mu}{2m_N}G_P(Q^2)\right]\gamma_5 u_N(p,s),$$

Induced pseudoscalar FF

$$\langle N(p',s')|P|N(p,s)\rangle = \bar{u}_N(p',s')\; G_5(Q^2)\,\gamma_5 u_N(p,s),$$

$$P^{\text{isov}} = \bar{u}\gamma_5 u - \bar{d}\gamma_5 d$$

Pseudoscalar FF

Two important operator relations are

i) $\partial^\mu A_\mu = 2m_q P$ *ii)* $\partial^\mu A_\mu = F_\pi m_\pi^2 \psi_\pi$ $\Rightarrow$ *iii)* $\psi_\pi = \frac{2m_q}{F_\pi m_\pi^2}P$

i) The axial Ward-Takahashi identity leads to the partial conservation of the axial-vector current (PCAC)

ii) The spontaneous breaking of chiral symmetry relates the axial-vector current to the pion field ψ_π

Continuum limit of (induced) pseudoscalar FFs

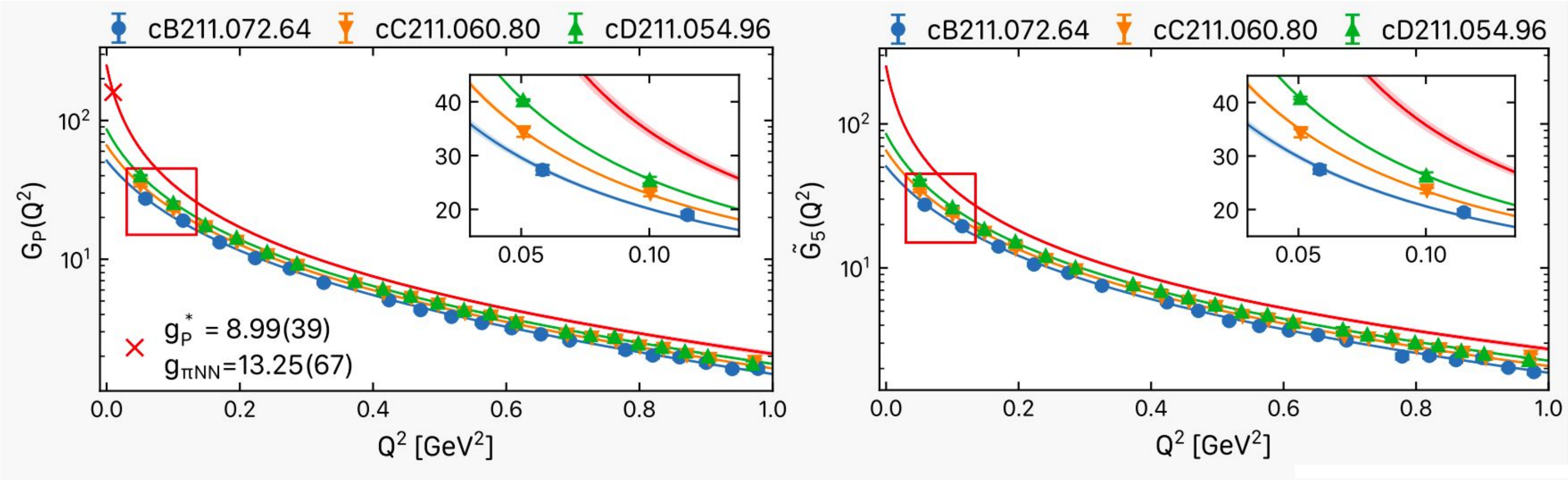

- We observe significant cut-off effects on both form factors
- Combined fit of both form factor with common pole
- Data highly correlated and ratio grows linearly in Q^2 $\frac{4m_N}{m_\pi^2}\frac{m_q G_5(Q^2)}{G_P(Q^2)}$

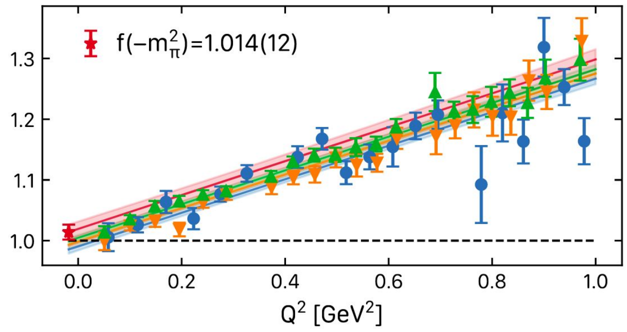

The PCAC and PPD relations

$$\langle N(p',s')|A_\mu|N(p,s)\rangle = \bar{u}_N(p',s')\left[\gamma_\mu G_A(Q^2) - \frac{Q_\mu}{2m_N}G_P(Q^2)\right]\gamma_5 u_N(p,s)$$

∂^μ

$$\langle N(p',s')|\partial^\mu A_\mu|N(p,s)\rangle = \bar{u}_N(p',s')\left[2m_N G_A(Q^2) - \frac{Q^2}{2m_N}G_P(Q^2)\right]\gamma_5 u_N(p,s)$$

$$\langle N(p',s')|P|N(p,s)\rangle = \bar{u}_N(p',s')\; G_5(Q^2)\,\gamma_5 u_N(p,s)$$

i) $\partial^\mu A_\mu = 2m_q P$

PCAC

$$\boxed{G_A(Q^2) - \frac{Q^2}{4m_N^2}G_P(Q^2) = \frac{m_q}{m_N}G_5(Q^2)}$$

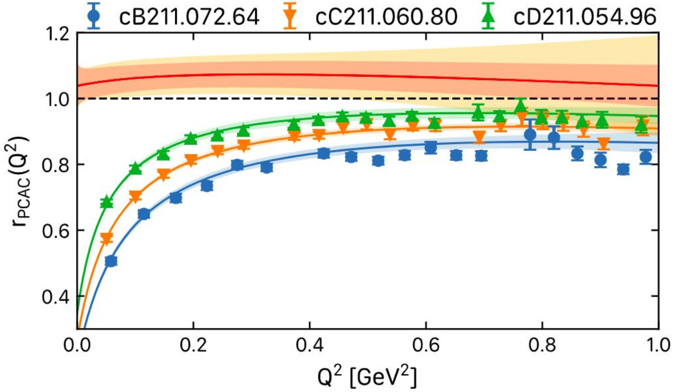

$$r_{\rm PCAC}(Q^2) = \frac{\frac{m_q}{m_N}G_5(Q^2) + \frac{Q^2}{4m_N^2}G_P(Q^2)}{G_A(Q^2)}$$

The PCAC and PPD relations

$$\langle N(p',s')|A_\mu|N(p,s)\rangle = \bar{u}_N(p',s')\left[\gamma_\mu G_A(Q^2) - \frac{Q_\mu}{2m_N}G_P(Q^2)\right]\gamma_5 u_N(p,s)$$

∂^μ

$$\langle N(p',s')|\partial^\mu A_\mu|N(p,s)\rangle = \bar{u}_N(p',s')\left[2m_N G_A(Q^2) - \frac{Q^2}{2m_N}G_P(Q^2)\right]\gamma_5 u_N(p,s)$$

$$\langle N(p',s')|P|N(p,s)\rangle = \bar{u}_N(p',s')\; G_5(Q^2)\,\gamma_5 u_N(p,s)$$

i) $\partial^\mu A_\mu = 2m_q P$

PCAC

$$\boxed{G_A(Q^2) - \frac{Q^2}{4m_N^2}G_P(Q^2) = \frac{m_q}{m_N}G_5(Q^2)}$$

iii) $\psi_\pi = \frac{2m_q}{F_\pi m_\pi^2}P$

$$\langle N(p',s')|\psi_\pi|N(p,s)\rangle = \bar{u}_N(p',s')\;\underbrace{(m_\pi^2+Q^2)^{-1}}_{\text{Pole at } Q^2=-m_\pi^2}G_{\pi NN}(Q^2)\,\gamma_5 u_N(p,s)$$

PPD

$$\boxed{m_q G_5(Q^2) = \frac{F_\pi m_\pi^2}{m_\pi^2+Q^2}G_{\pi NN}(Q^2)}$$

PPD = Pion-pole dominance

The Goldberger-Treiman relation

$$m_q G_5(Q^2) = \frac{F_\pi m_\pi^2}{m_\pi^2+Q^2} G_{\pi NN}(Q^2)$$

$$G_A(Q^2) - \frac{Q^2}{4m_N^2} G_P(Q^2) = \frac{F_\pi m_\pi^2}{m_N(m_\pi^2+Q^2)} G_{\pi NN}(Q^2)$$

$$\lim_{Q^2\to -m_\pi^2} (Q^2 + m_\pi^2) m_q G_5(Q^2) = F_\pi m_\pi^2 g_{\pi NN}$$

$$\lim_{Q^2\to -m_\pi^2} (Q^2 + m_\pi^2) G_P(Q^2) = 4 m_N F_\pi g_{\pi NN}$$

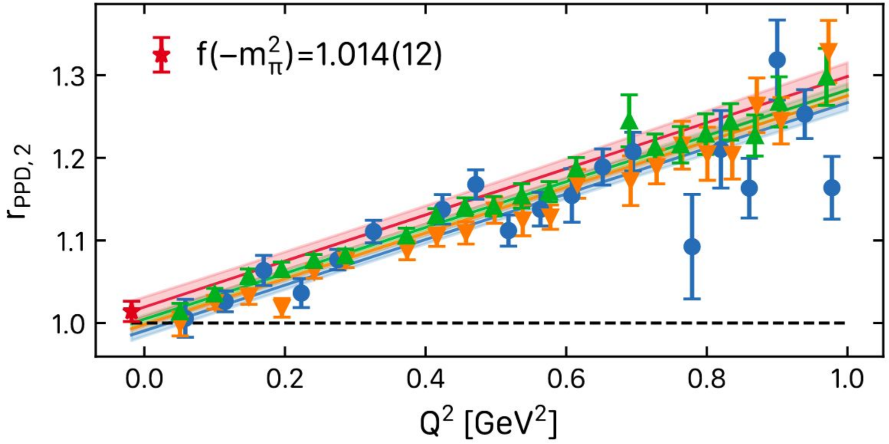

with $g_{\pi NN} = G_{\pi NN}(-m_\pi^2)$

$$r_{\mathrm{PPD},2}(Q^2) = \frac{4m_N}{m_\pi^2} \frac{m_q G_5(Q^2)}{G_P(Q^2)}$$

The slope is connected to the GT discrepancy

$$\Delta_{\mathrm{GT}} = 1 - \frac{g_A m_N}{g_{\pi NN} F_\pi} = 2.13(38)\% \approx 2\%$$

And our results on ElectroMagnetic FFs

$$\langle N(p',s')|j_\mu|N(p,s)\rangle = \sqrt{\frac{m_N^2}{E_N(\vec{p}')E_N(\vec{p})}}\,\bar{u}_N(p',s')\left[\gamma_\mu F_1(q^2) + \frac{i\sigma_{\mu\nu}q^\nu}{2m_N}F_2(q^2)\right]u_N(p,s)$$

$$G_E(q^2) = F_1(q^2) + \frac{q^2}{4m_N^2}F_2(q^2)$$

$$G_M(q^2) = F_1(q^2) + F_2(q^2)$$

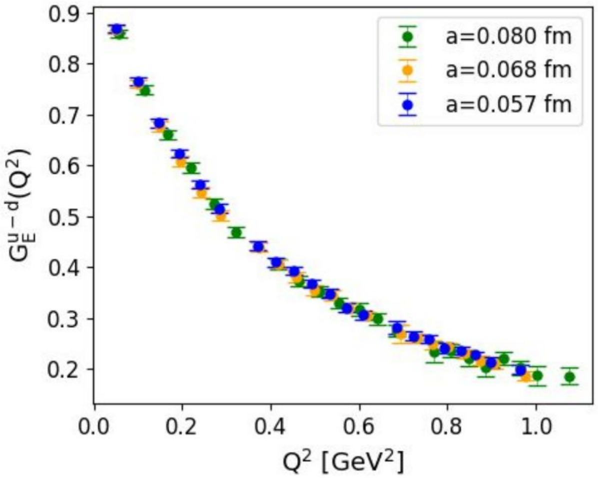

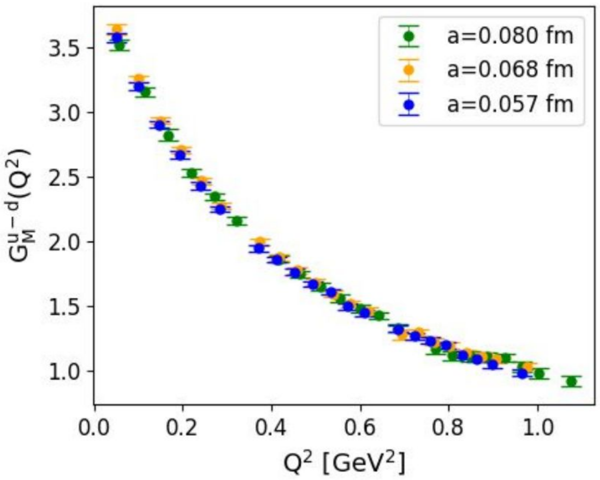

- No sizeable cut-off effects
- Isovector combination u-d needed for neutron β-decay

Isoscalar u+d combinations

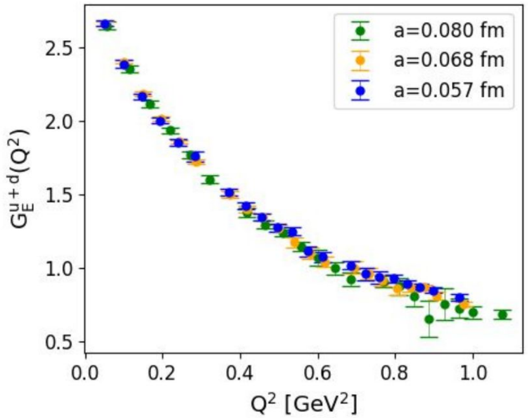

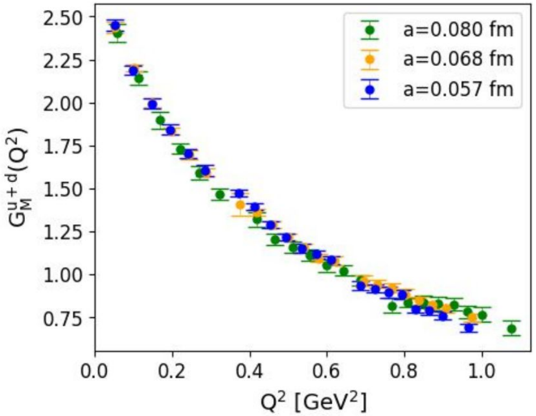

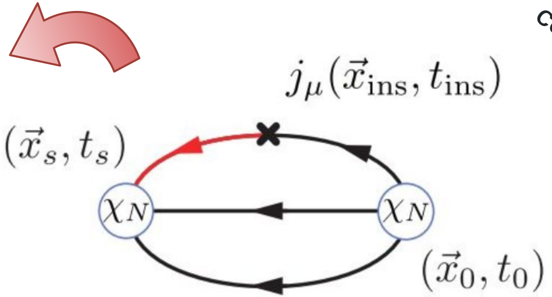

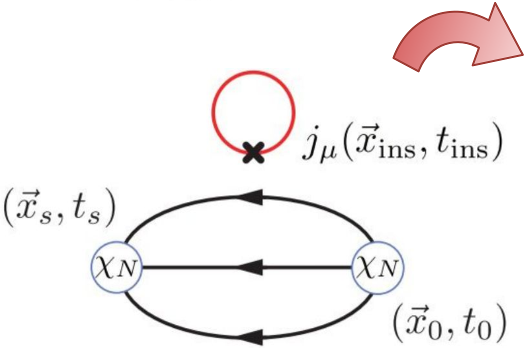

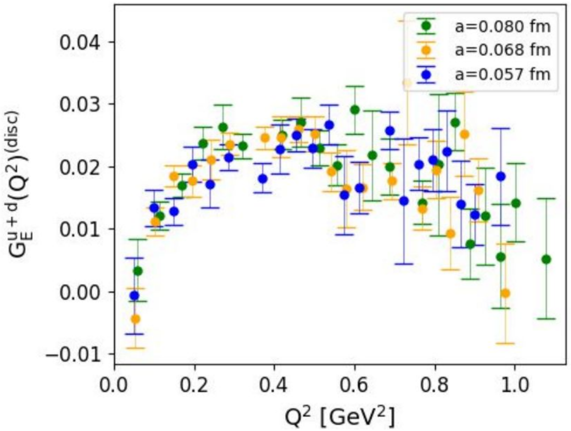

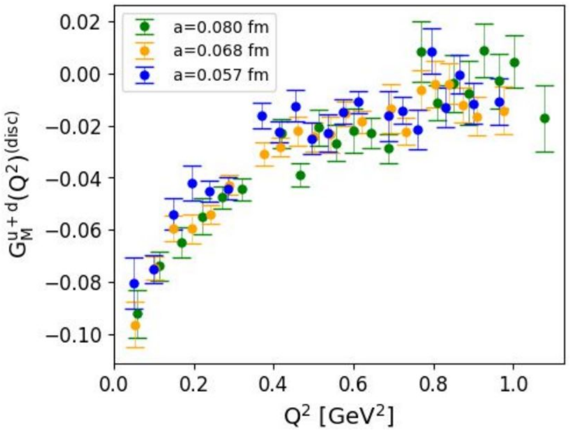

Proton and Neutron EM FFs

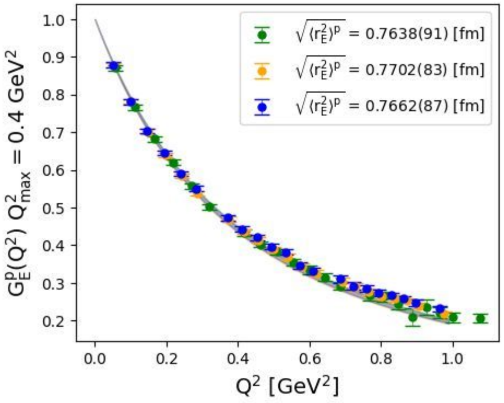

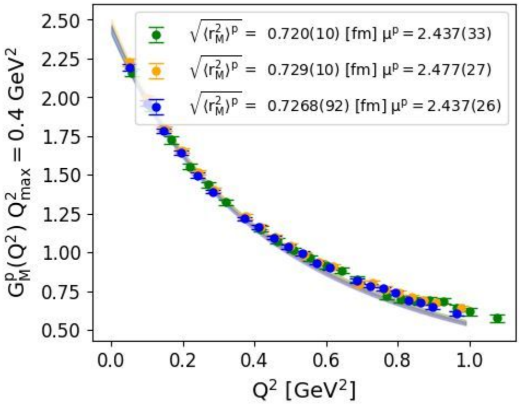

$$G^p(Q^2) = \frac{1}{2}\left[\frac{G^{u+d}(Q^2)}{3} + G^{u-d}(Q^2)\right]$$

$$G_E^p(0) = 1 \quad G_M^p(0) = \mu_p$$

$$G^n(Q^2) = \frac{1}{2}\left[\frac{G^{u+d}(Q^2)}{3} - G^{u-d}(Q^2)\right]$$

$$G_E^n(0) = 0 \quad G_M^n(0) = \mu_n$$

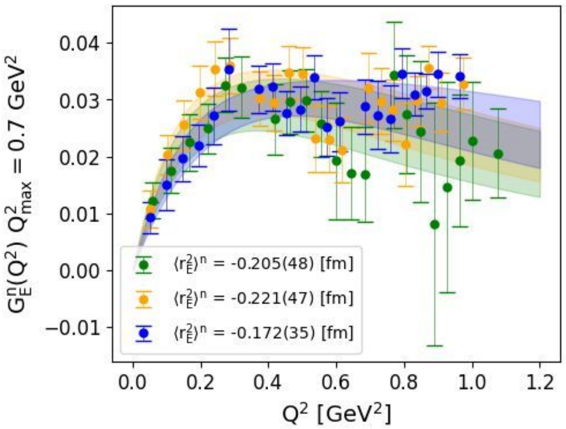

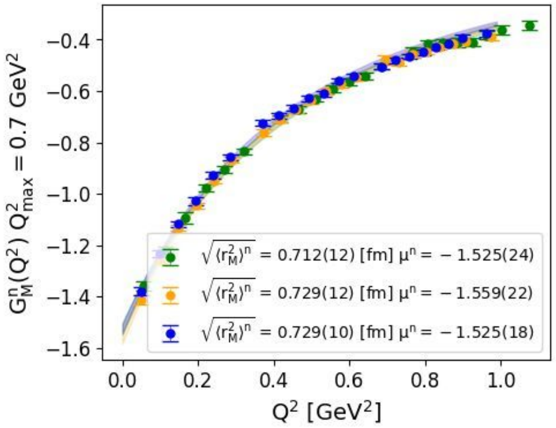

Comparison with other studies

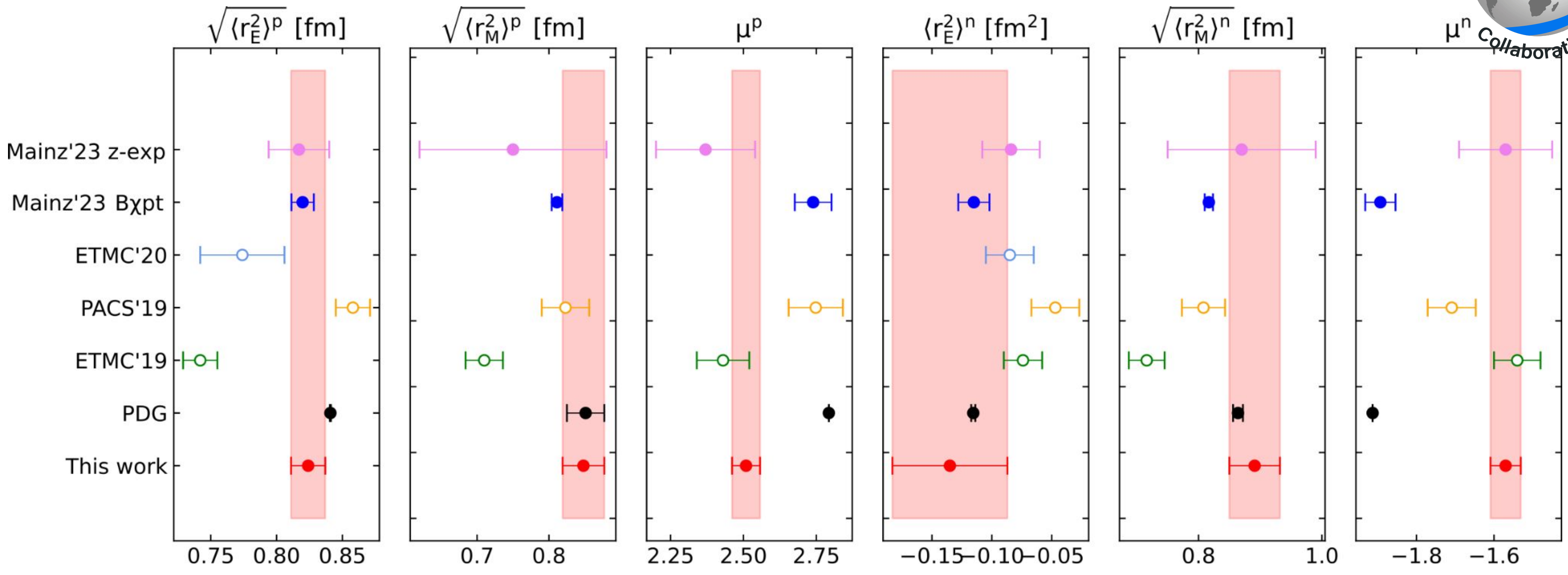

- Good agreement for radii with PDG
- Tension of our results in magnetic moments

PRELIMINARY

Thank you for you attention!

Results on nucleon isovector axial, induced pseudoscalar, and pseudoscalar form factors (FF)

- Three physical point ensemble
- Thorough excited state analysis
- Combined fit of Q^2-dependence and continuum limit

https://arxiv.org/abs/2309.05774

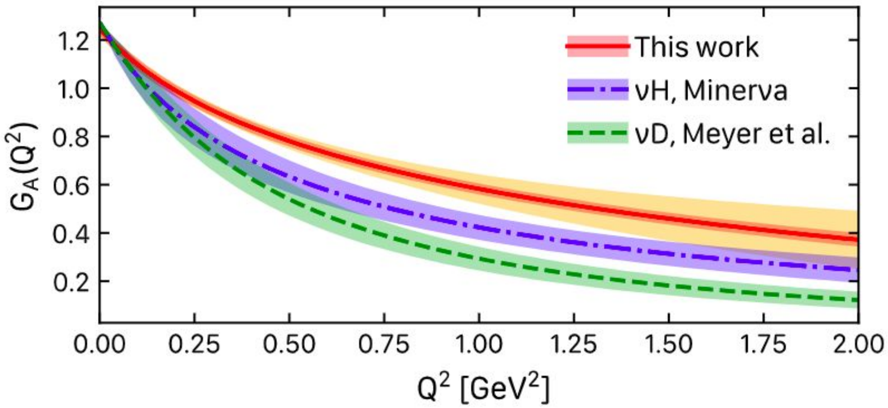

Nucleon axial and pseudoscalar form factors using twisted-mass fermion ensembles at the physical point

Constantia Alexandrou,[1,2] Simone Bacchio,[2] Martha Constantinou,[3] Jacob Finkenrath,[4,2] Roberto Frezzotti,[5] Bartosz Kostrzewa,[6] Giannis Koutsou,[2] Gregoris Spanoudes,[1] and Carsten Urbach[7]

(Extended Twisted Mass Collaboration)

[1] *Department of Physics, University of Cyprus, P.O. Box 20537, 1678 Nicosia, Cyprus*
[2] *Computation-based Science and Technology Research Center, The Cyprus Institute, Nicosia, Cyprus*
[3] *Department of Physics, Temple University, Philadelphia, PA 19122 - 1801, USA*
[4] *University of Wuppertal, Wuppertal, Germany*
[5] *Dipartimento di Fisica and INFN, Università di Roma "Tor Vergata", Via della Ricerca Scientifica 1, I-00133 Roma, Italy*
[6] *High Performance Computing and Analytics Lab, Rheinische Friedrich-Wilhelms-Universität Bonn, Friedrich-Hirzebruch-Allee 8, 53115 Bonn, Germany*
[7] *HISKP (Theory), Rheinische Friedrich-Wilhelms-Universität Bonn, Nussallee 14-16, 53115 Bonn, Germany*

(Dated: October 28, 2023)

We compute the nucleon axial and pseudoscalar form factors using three $N_f = 2+1+1$ twisted mass fermion ensembles with all quark masses tuned to approximately their physical values. The values of the lattice spacings of these three physical point ensembles are 0.080 fm, 0.068 fm and 0.057 fm, and spatial sizes 5.1 fm, 5.44 fm, and 5.47 fm, respectively, yielding $m_\pi L > 3.6$. Convergence to the ground state matrix elements is assessed using multi-state fits. We study the momentum dependence of the three form factors and check the partially conserved axial-vector current (PCAC) hypothesis and the pion pole dominance (PPD). We show that in the continuum limit, the PCAC and PPD relations are satisfied. We also show that the Goldberger-Treimann relation is approximately fulfilled and determine the Goldberger-Treiman discrepancy. We find for the nucleon axial charge $g_A = 1.245(28)(14)$, for the axial radius $\langle r_A^2 \rangle = 0.339(48)(06)$ fm^2, for the pion-nucleon coupling constant $g_{\pi NN} \equiv \lim_{Q^2 \to -m_\pi^2} G_{\pi NN}(Q^2) = 13.25(67)(69)$ and for $G_P(0.88 m_\mu^2) \equiv g_P^* = 8.99(39)(49)$.

Backup slide - OS pion pole

$$\langle N(p', s')|P|N(p, s)\rangle \qquad P^{\text{isov}} = \bar{u}\gamma_5 u - \bar{d}\gamma_5 d$$

Connected neutral pion

Matrix elements couples to the Osterwalder-Seiler (OS) pion

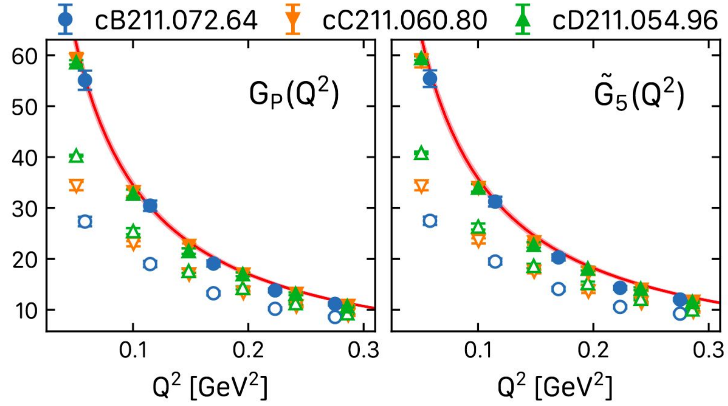

$$G_{\text{improved}}(Q^2, a^2) = \frac{Q^2 + m^2_{\pi,\text{OS}}}{Q^2 + m^2_{\pi,\text{TM}}} G_{\text{w pole}}(Q^2, a^2)$$

Charged pion

Ensemble	m_π^{pole} [MeV]	m_π^{TM} [MeV]	m_π^{OS} [MeV]
cB211.72.64	299.3(4.5)	140.2(2)	297.5(7)
cC211.60.80	266.7(3.2)	136.6(2)	248.9(5)
cD211.54.96	235.8(4.8)	140.8(3)	210.0(4)

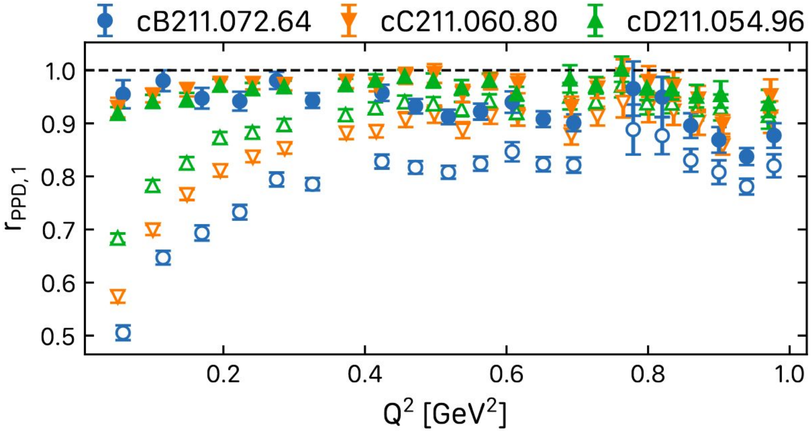

Backup slide - Comparison with experiments

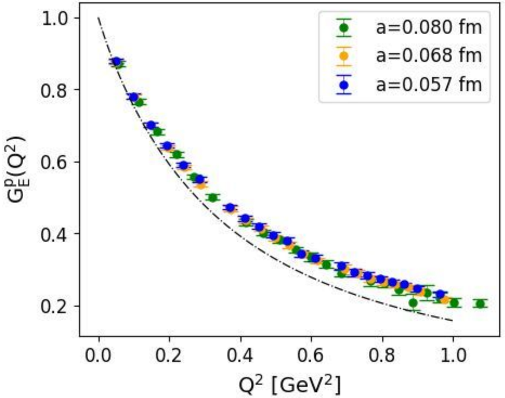

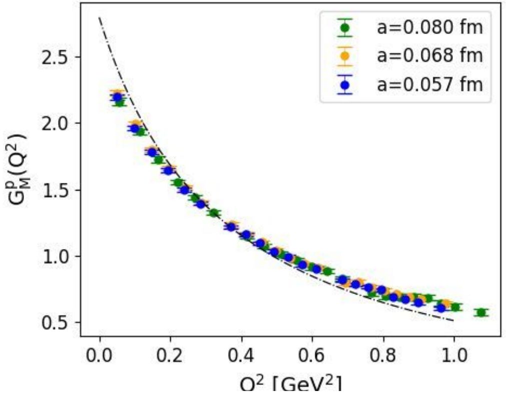

$$G^p(Q^2) = \frac{1}{2}\left[\frac{G^{u+d}(Q^2)}{3} + G^{u-d}(Q^2)\right]$$

$$G_E^p(0) = 1 \quad G_M^p(0) = \mu_p$$

$$G^n(Q^2) = \frac{1}{2}\left[\frac{G^{u+d}(Q^2)}{3} - G^{u-d}(Q^2)\right]$$

$$G_E^n(0) = 0 \quad G_M^n(0) = \mu_n$$